© 2016. Published by The Company of Biologists Ltd | Development (2016) 143, 1182-1191 doi:10.1242/dev.128934

RESEARCH ARTICLE

EFN-4 functions in LAD-2-mediated axon guidance in *Caenorhabditis elegans*

Bingyun Dong[1], Melinda Moseley-Alldredge[1,2], Alicia A. Schwieterman[3], Cory J. Donelson[3,*], Jonathan L. McMurry[3], Martin L. Hudson[3] and Lihsia Chen[1,2,‡]

ABSTRACT

During development of the nervous system, growing axons rely on guidance molecules to direct axon pathfinding. A well-characterized family of guidance molecules are the membrane-associated ephrins, which together with their cognate Eph receptors, direct axon navigation in a contact-mediated fashion. In *C. elegans*, the ephrin-Eph signaling system is conserved and is best characterized for their roles in neuroblast migration during early embryogenesis. This study demonstrates a role for the *C. elegans* ephrin EFN-4 in axon guidance. We provide both genetic and biochemical evidence that is consistent with the *C. elegans* divergent L1 cell adhesion molecule LAD-2 acting as a non-canonical ephrin receptor to EFN-4 to promote axon guidance. We also show that EFN-4 probably functions as a diffusible factor because EFN-4 engineered to be soluble can promote LAD-2-mediated axon guidance. This study thus reveals a potential additional mechanism for ephrins in regulating axon guidance and expands the repertoire of receptors by which ephrins can signal.

KEY WORDS: *C. elegans*, Ephrin, L1CAM, Axon guidance

INTRODUCTION

Neural circuitries underlying complex behaviors require precise neuronal connections that are formed during development. The specificity of these connections requires accurate axon pathfinding, which is controlled by many molecules, including growth factors, adhesion molecules, and long- and short-range guidance cues and their receptors. An important class of guidance cues are the ephrins, which are either glycosyl-phosphatidylinositol (GPI) linked or single-pass transmembrane proteins (Helmbacher et al., 2000; Luria et al., 2008; Wang et al., 2001). In mammals, the five GPI-linked 'A' class ephrins and the three transmembrane 'B' class ephrins act as short-range guidance cues that signal via their cognate A or B class Eph receptor tyrosine kinases. Classically, ephrins signal by forming *trans* interactions with Eph receptors on opposing tissues. These interactions generally result in repulsion when the associated ephrins are proteolytically released by ADAM (A disintegrin and metalloprotease) proteins (Egea and Klein, 2007; Hattori et al., 2000; Janes et al., 2005). The level of repulsion or adhesion between the two opposing tissues can be modulated by a variety of mechanisms, including *cis* interactions between ephrin and the Eph receptor (Hornberger et al., 1999; Kao and Kania, 2011).

[1]Department of Genetics, Cell Biology & Development, University of Minnesota, Minneapolis, MN 55455, USA. [2]Developmental Biology Center, University of Minnesota, Minneapolis, MN 55455, USA. [3]Department of Molecular and Cellular Biology, Kennesaw State University, Kennesaw, GA 30144, USA.
*Present address: Department of Biological Sciences, University of South Carolina, Columbia, SC 29203, USA.

‡Author for correspondence (chenx260@umn.edu)

Received 23 July 2015; Accepted 12 February 2016

Ephrins and Eph receptors are also conserved in *C. elegans*, whose genome contains four genes (*efn-1* to *efn-4*) that encode GPI-linked ephrins and a single gene (*vab-1*) that encodes an Eph receptor (Chin-Sang et al., 1999, 2002; George et al., 1998; Wang et al., 1999). Although a role in axon guidance has been demonstrated for the VAB-1/Eph receptor (Boulin et al., 2006; Mohamed and Chin-Sang, 2006) and the EFN-1 ephrin (Grossman et al., 2013), the *C. elegans* ephrins and VAB-1 have been best characterized for their role in embryonic morphogenesis. EFN-1, EFN-2 and EFN-3 function together in epidermal cell organization, signaling through VAB-1 (Chin-Sang et al., 1999; Wang et al., 1999). Although EFN-4 also functions in epidermal morphogenesis, its role appears to be predominantly independent of VAB-1. Indeed, epidermal morphogenesis defects in *efn-4* null embryos are synergistically enhanced in a *vab-1* null background, consistent with each protein functioning in parallel pathways (Chin-Sang et al., 2002). EFN-4 also plays a major role in morphogenesis of the male tail, a process in which VAB-1 and the other three ephrins have not been reported to participate (Ikegami et al., 2004; Nakao et al., 2007). More recently, EFN-4 was revealed to have a role in promoting axon branching that is also partially independent of VAB-1 (Schwieterman et al., 2016). These studies collectively suggest the presence of additional receptors for ephrins besides the Eph receptors.

Here, we present genetic evidence showing that EFN-4 plays a role in axon guidance, probably by acting as a soluble factor. We provide both genetic and biochemical data that is consistent with LAD-2, a non-canonical L1 cell adhesion molecule, acting as an EFN-4 receptor.

RESULTS

efn-4 functions in the same genetic pathway as *lad-2* in axon guidance

Prior studies established EFN-4 and MAB-20/semaphorin as essential for male tail morphogenesis (Ikegami et al., 2004; Nakao et al., 2007). In these studies, EFN-4 and MAB-20 are shown to function in common pathways. Although MAB-20 signaling is mediated by the PLX-2 plexin receptor, it is not clear how the EFN-4 signal is communicated. In another genetic study, both EFN-4 and MAB-20 are shown to function together in embryonic epidermal morphogenesis (Chin-Sang et al., 2002). We previously showed that MAB-20 functions to direct axon pathfinding of the SDQL, SDQR, SMD and PLN neurons; MAB-20 signal is mediated via the PLX-2/plexin receptor and LAD-2, a non-canonical L1 cell adhesion molecule (L1CAM) that functions as a MAB-20 co-receptor and is expressed in these neurons (Wang et al., 2008). Given that EFN-4 and MAB-20 function in common processes and the fact that *efn-4* is expressed in the nervous system, including several lateral and tail neurons (Chin-Sang et al., 2002; also see Fig. S1), we tested the possibility that EFN-4 might also direct pathfinding of axons that rely on MAB-20, PLX-2 and

Development (2016) 143, 1182-1191 doi:10.1242/dev.128934

LAD-2. Using a *lad-2* transcriptional GFP reporter, we examined the axon trajectories of the SDQL, SDQR, SMD and PLN neurons in *efn-4* null animals and observed significant abnormalities (Fig. 1). In particular, the SDQL axon exhibited two phenotypes that were strikingly similar to those observed in *lad-2* null animals (Fig. 1Aii-Av). In wild-type animals, the SDQL neuron extended a single dorsal axon (Fig. 1Ai, double-headed arrow) that joins the lateral nerve cord, along which it migrates anteriorly before making a second dorsal turn (Fig. 1Ai, arrow) to join the sublateral nerve cord, along which it continues to migrate anteriorly towards the nerve ring. In 37% of *efn-4* null animals, the SDQL axon failed to make the second dorsal turn, migrating ventrally instead (Fig. 1Aiv, arrow). The *efn-4* SDQL neuron also often extended an additional axon from the cell body that typically migrates in the opposite direction to the primary axon (Fig. 1Av). These shared axon defects in *efn-4* and *lad-2* null animals suggest that both genes function in the same genetic pathway. Consistent with this hypothesis, the observed SDQL, SDQR, SMD and PLN axon defects in *efn-4; lad-2* double mutant animals are no worse than those observed in *lad-2* single mutant animals (Fig. 1B).

To evaluate whether VAB-1, the sole *C. elegans* Eph receptor, participates with EFN-4 in guiding axon migration, we first examined *vab-1* null animals for similar defects in the aforementioned sublateral axons. Although the penetrance of PLN axon defects in *vab-1* null animals is similar to *efn-4* null animals, we observed a more modest level of SMD, SDQL and SDQR axon guidance defects in *vab-1* null animals compared with *efn-4* null animals (Fig. 1B). These results reveal a pathfinding role for *vab-1* in these sublateral axons. Owing to synthetic embryonic lethality in *vab-1; efn-4* mutant backgrounds (Chin-Sang et al., 2002), we were unable to evaluate whether *efn-4* and *vab-1* function in the same pathway. But the more penetrant SDQL, SDQR and SMD axon defects in *efn-4* animals suggest that EFN-4 can function, at least partially, independent of VAB-1.

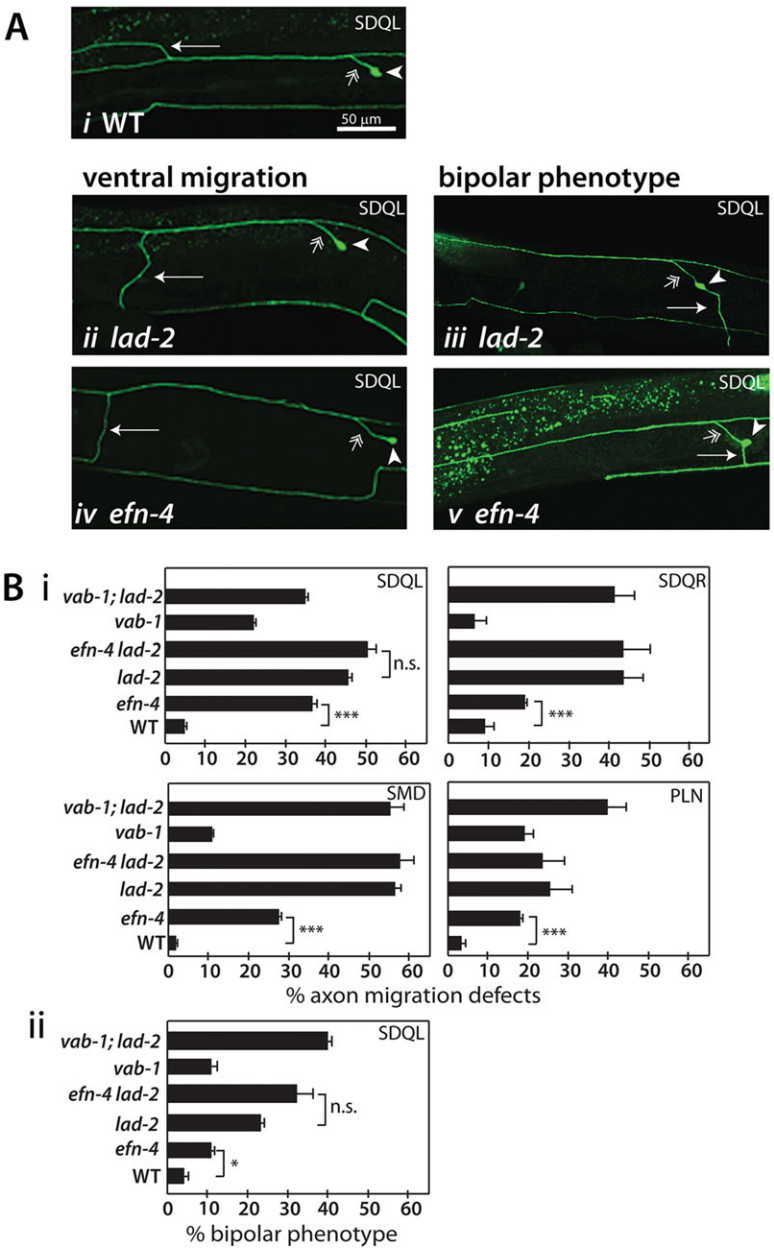

Fig. 1. *efn-4* animals exhibit abnormal axon trajectories in *lad-2*-expressing neurons. (A) Confocal micrographs of the SDQL neuron (arrowhead) in adult wild-type, *lad-2* and *efn-4* animals expressing P*lad-2*::*gfp*; left lateral view. The wild-type SDQL neuron (Ai) extends a single dorsal axon (double-headed arrow) that migrates anteriorly before making a dorsal turn (arrow) and navigating anteriorly again. The SDQL axon in *efn-4*(*bx80*) animals exhibit strikingly similar abnormalities to those observed in *lad-2* (*tm3056*) animals. Instead of a second dorsal migration, the SDQL axon often navigates ventrally (arrow) in *lad-2* (Aii) and *efn-4* animals (Aiv). The SDQL neuron sometimes displays a bipolar phenotype, extending a second axon that migrates ventrally (arrow) in *lad-2* (Aiii) and *efn-4* animals (Av). (B) Quantitation of abnormal axon pathfinding (Bi) observed in SDQL as well as additional *lad-2*-expressing neurons, SDQR, SMD and PLN and (Bii) bipolar phenotype in SDQL. Error bars indicate standard error of proportion of three sample sets, where n=100 animals for each set. *P<0.05, ***P<0.0005. n.s., not significant.

Development (2016) 143, 1182-1191 doi:10.1242/dev.128934

To determine how *vab-1* functions relative to *lad-2*, we examined axon defects in *vab-1; lad-2* animals. PLN defects in *vab-1; lad-2* animals showed increased penetrance (Fig. 1B) that is consistent with additive effects, suggesting that *vab-1* and *lad-2* function in distinct pathways in PLN pathfinding. However, SDQL, SDQR and SMD axon defects in *vab-1; lad-2* animals showed either some reduction or no significant difference in penetrance compared with that in *lad-2* animals, consistent with both genes having antagonistic roles or sharing a common pathway.

efn-4 functions in a distinct pathway from *mab-20* and *plx-2* in LAD-2-mediated axon guidance

As the SDQL defects in both *efn-4* and *lad-2* null mutants are strikingly similar, we focused on the SDQL neuron as a model system to dissect how *efn-4* mediates in axon guidance. To assess how *efn-4* functions relative to *mab-20* and *plx-2*, we compared SDQL axons in each single mutant strain relative to *mab-20; plx-2*, *mab-20; efn-4* and *plx-2; efn-4* animals (Fig. 2). In agreement with *mab-20* and *plx-2* functioning in the same pathway (Ikegami et al., 2004; Nakao et al., 2007; Wang et al., 2008), *mab-20; plx-2* animals exhibited similar levels of SDQL axon defects as *mab-20* and *plx-2* single mutant animals (Fig. 2 and Wang et al., 2008). By contrast, the penetrance of SDQL defects in *mab-20; efn-4* and *plx-2; efn-4* animals were increased over *mab-2*, *plx-2* or *efn-4* null animals, consistent with *efn-4* functioning in a distinct pathway from *mab-20* and *plx-2*. In analyzing how all three genes function relative to *lad-2*, our genetic data indicate that loss of *mab-20*, *plx-2* or *efn-4* function does not enhance SDQL axon defects in *lad-2* animals (Fig. 2), thus revealing that each of the three genes functions in the same pathway as *lad-2*.

LAD-2 biochemically interacts with EFN-4

Our genetic results suggest the presence of at least two distinct pathways – *mab-20* and *efn-4* – that converge on LAD-2 to promote SDQL axon guidance. Because LAD-2 is an established co-receptor for the MAB-20 guidance cue (Wang et al., 2008), we hypothesized that LAD-2 might also act as a receptor for EFN-4 and thus should physically interact with EFN-4. To evaluate this possibility, we performed co-immunoprecipitation (co-IP) assays on lysates of HEK293T cells co-transfected with FLAG::EFN-4 and LAD-2::HA. We detected LAD-2::HA in anti-FLAG immunoprecipitates as determined by western blot analysis using anti-HA antibodies (Fig. 3A). By contrast, no LAD-2::HA was detected in anti-FLAG immunoprecipitates performed on cells co-transfected with LAD-2::HA and control FLAG vector or with FLAG::EFN-4 and control HA vector. These results indicate that LAD-2 and EFN-4 can biochemically interact.

To assess the specificity of this biochemical interaction, we performed co-IP assays assessing the ability of EFN-4 to interact with MAB-20 and two immunoglobulin superfamily cell adhesion molecules (IgCAMs): RIG-3, which also has axon guidance roles (Schwarz et al., 2009) and SAX-7, the canonical *C. elegans* L1CAM (Sasakura et al., 2005; Wang et al., 2005). These co-IP assays failed to reveal an EFN-4 interaction with either MAB-20 or RIG-3, confirming the specificity of the interaction between EFN-4 and LAD-2 (Fig. S2A) and agreeing with our genetic result that

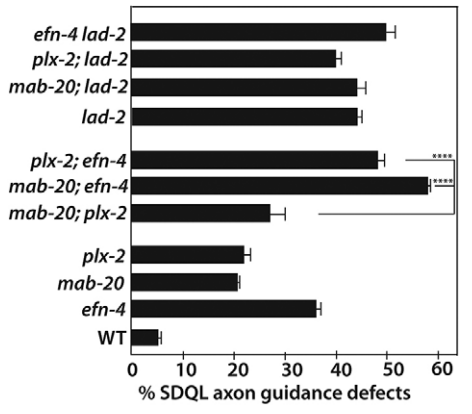

Fig. 2. Genetic analysis reveals that *efn-4* and *mab-20* function in distinct pathways. Quantitation of abnormal SDQL axon guidance observed in *efn-4*, *mab-20*, *plx-2* and *lad-2* single and double mutant strains. Error bars indicate standard error of proportion of three sample sets, where *n*=100 animals for each set. ****P<0.0001.

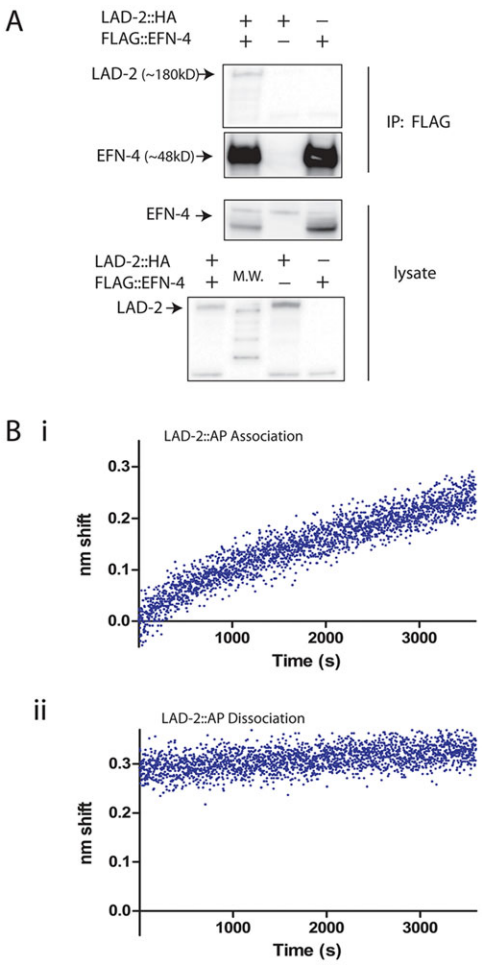

Fig. 3. LAD-2 can biochemically interact with EFN-4 as determined by co-immunoprecipitation assays and biolayer interferometry. (A) A western blot showing results of a co-immunoprecipitation assay performed on lysates of HEK293T cell expressing HA-tagged LAD-2 (LAD-2::HA) and/or FLAG-tagged EFN-4 (FLAG::EFN-4). M.W., molecular weight markers. (B) BioLayer Interferometry (BLI) reveals a fast-on, slow-off binding interaction between LAD-2-AP and EFN-4-Fc. A BLI probe against human Fc was used to capture secreted EFN-4-Fc in parallel with a secreted Fc control. After baseline measurements in Opti-MEM medium alone, the captured EFN-4 ligand was dipped into tissue culture supernatant from cells transiently transfected with a secreted LAD-2-AP expression plasmid during the association phase (Bi), then dipped into Opti-MEM during the dissociation phase (Bii). BLI measurements of the Fc control interaction with LAD-2-AP showed no appreciable binding and were used to correct for instrument drift. The negligible dissociation observed in Bii is consistent with a high-affinity interaction between EFN-4 and LAD-2.

Development (2016) 143, 1182-1191 doi:10.1242/dev.128934

efn-4 and *mab-20* function in distinct genetic pathways. However, the co-IP assays identified an interaction between EFN-4 and SAX-7 – a result that is not surprising because SAX-7 and LAD-2 share a highly conserved extracellular domain (Chen and Zhou, 2010; Wang et al., 2008).

To further evaluate the binding of EFN-4 to LAD-2, we used biolayer interferometry (BLI), an optical biosensing technique similar to surface plasmon resonance that can measure the association and disassociation of biomolecules (Abdiche et al., 2008; Wartchow et al., 2011; Wilson et al., 2010). In BLI assays, we immobilized EFN-4::Fc or the Fc control onto an anti-human Fc capture probe, after which we immersed the probe into conditioned tissue culture medium isolated from HEK293T cells transiently expressing the LAD-2 extracellular domain fused to alkaline phosphatase (LAD-2::AP). The BLI measurements collected over a span of >3000 s are indicative of an association between LAD-2::AP and EFN-4::Fc (Fig. 3B). By contrast, the Fc control showed no significant association. To qualitatively evaluate the strength of the LAD-2ECD::AP association with EFN-4::Fc, the probe was subsequently immersed in naive tissue culture medium. BLI measurements taken for >3000 s revealed little protein dissociation, indicative of a strong affinity between LAD-2::AP and EFN-4. These BLI analyses confirm that EFN-4 and LAD-2 can directly bind each other. BLI measurements were also performed to assess the interaction of RIG-3ECD::AP with EFN-4::Fc; no significant interaction between EFN-4 and RIG-3 was found (Fig. S2B), in agreement with our co-IP results.

EFN-4 can function non-cell autonomously to mediate axon guidance

Ephrins can form *cis* or *trans* interactions with their cognate Eph receptors to modulate contact-dependent axon migration (Hornberger et al., 1999; Kao and Kania, 2011; Rashid et al., 2005). As a GPI-linked molecule, EFN-4 could function in *cis* with LAD-2 during SDQL axon migration or in *trans*, presented from adjacent tissues. Throughout its entire navigation, the SDQL axon extends along the hyp7 epidermal cell and is adjacent to the dorsal body-wall muscles, which form the dorsal boundary that the axon does not trespass beyond (Fig. 4A; White et al., 1986). On the basis of EFN-4::GFP expression from the *juIs109* transgene (Chin-Sang et al., 2002), it was not clear whether EFN-4 is expressed in SDQL neurons (Fig. S1). To determine whether EFN-4 is required in the SDQL neuron, we tested for EFN-4 expression driven by the *lad-2* promoter to rescue SDQL cell defects in *efn-4* null animals. We observed significant rescue of SDQL pathfinding (Fig. 4B), consistent with a cell-autonomous role for EFN-4. To test whether EFN-4 in adjacent tissues is also required for SDQL axon pathfinding, we expressed EFN-4 in either hyp7 cells or body-wall muscles under the control of the *dpy-7* or *myo-3* promoter, respectively. Both promoters drive gene expression in the respective tissues in embryos, larvae and adults (Fire and Waterston, 1989; Gilleard et al., 1997; Okkema et al., 1993), thus EFN-4 would be present when the SDQL axon initiates extension. We observed significant SDQL cell rescue with EFN-4 expression in either hyp7 cells or body-wall muscles (Fig. 4B), demonstrating that EFN-4 can act both cell autonomously and non-cell autonomously and that EFN-4 expression in any of these tissues is sufficient to direct SDQL axon pathfinding.

To further probe the non-cell autonomous action of EFN-4, we assessed whether EFN-4 expression in remote cells, such as the RID and touch receptor mechanosensory neurons (Fig. 5A), could influence SDQL axon pathfinding. We used the *mir-48* (Li et al., 2005; Wang et al., 2008) and *mec-7* promoters (Kim et al., 1999) to express sustained levels of EFN-4 in the RID and touch receptor mechanosensory neurons. RID is an embryonically derived neuron whose axon is located in the dorsal nerve cord whereas axons of the mechanosensory neurons, particularly PLM and PVM, are ventral to the SDQL cell body and axon. Importantly, the axons of these neurons are fully extended and already express EFN-4 by the time the SDQL neuron initiates axon extension (White et al., 1986). EFN-4 expression in either RID or the mechanosensory neurons also rescues *efn-4* SDQL cell defects (Fig. 5B), revealing that EFN-4 expression in a distant tissue can direct SDQL axon guidance.

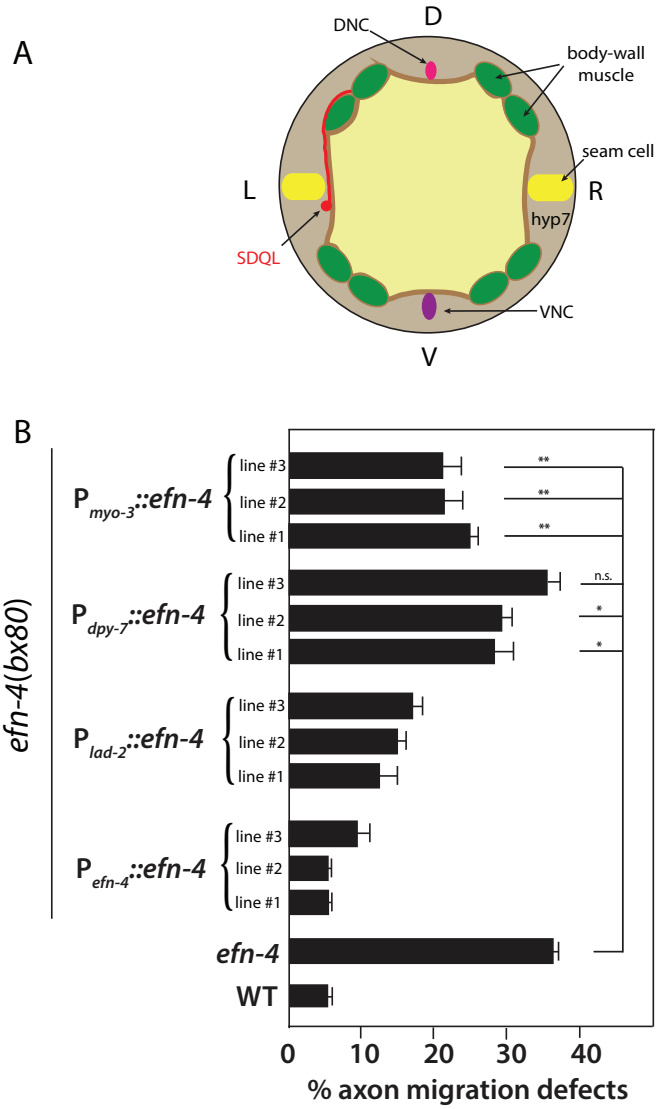

Fig. 4. *efn-4* can function non-cell autonomously to regulate SDQL axon guidance. (A) Schematic of a *C. elegans* mid-body cross section, showing the SDQL cell body and axon relative to other tissues. The SDQL neuron extends a single dorsal axon from its cell body, migrating anteriorly before making a dorsal turn until the axon reaches the left dorsal body-wall muscle, at which point it migrates anteriorly. VNC, ventral nerve cord; DNC, dorsal nerve cord. (B) Percentage of animals showing abnormal SDQL trajectories in different genetic backgrounds and in *efn-4*(*bx80*) transgenic animals expressing *efn-4* in different tissues with the use of tissue-specific promoters. In analyzing the effects of each tissue-specific *efn-4* expression on SDQL axon migration, we examined three independent transgenic lines. Error bars indicate standard error of proportion of three sample sets, where n=100 animals for each set. *P<0.05, **P<0.01; n.s., not significant.

Development (2016) 143, 1182-1191 doi:10.1242/dev.128934

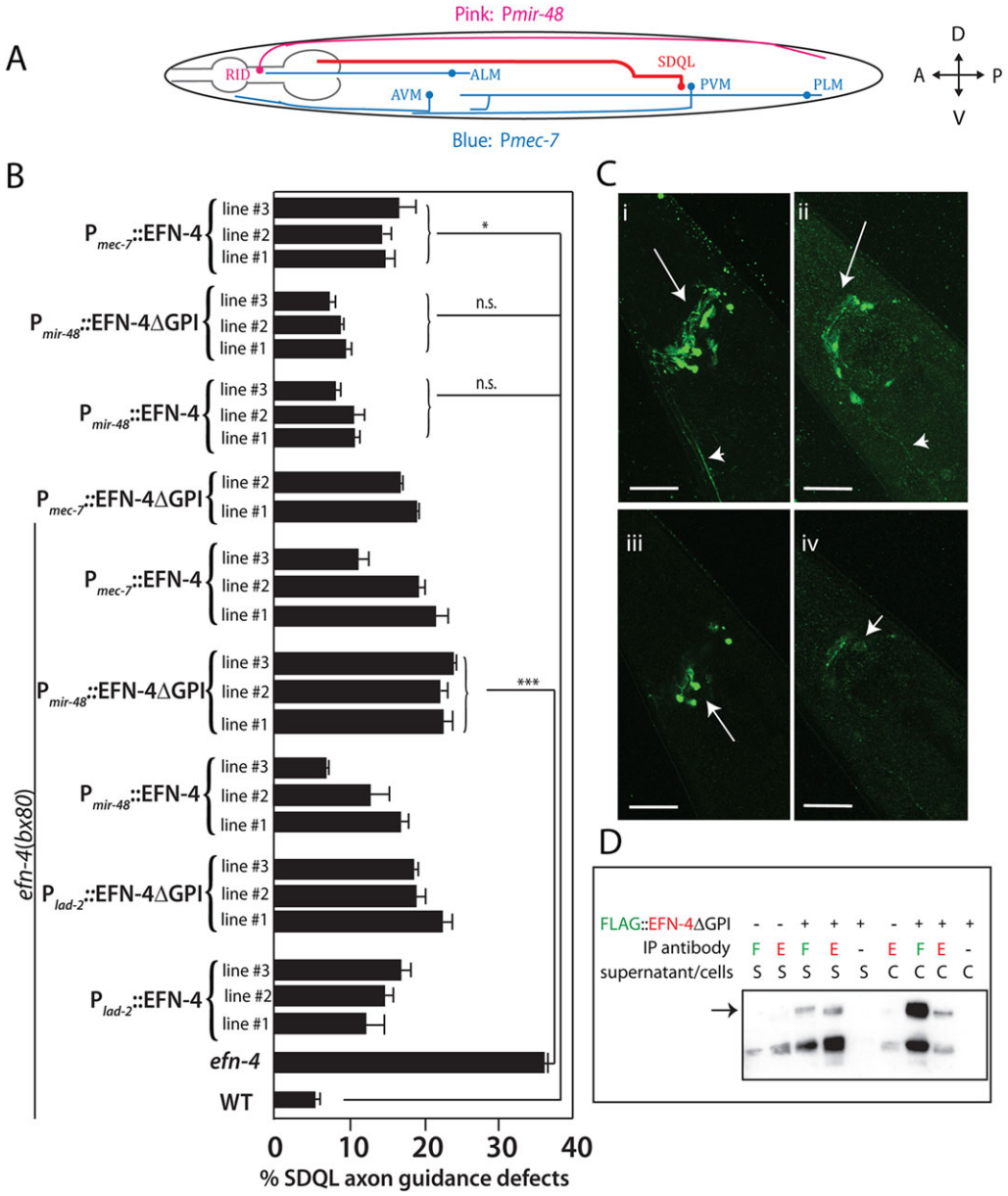

Fig. 5. Membrane association of EFN-4 is not required for EFN-4-mediated SDQL axon guidance. (A) A schematic showing SDQL axon trajectory (red) relative to those of the RID (pink) and several mechanosensory (blue) neurons. (B) Quantitation of SDQL neuron defects in *efn-4*(*bx80*) and wild-type animals expressing EFN-4 or EFN-4ΔGPI in SDQL, RID and mechanosensory neurons. We examined three independent transgenic lines to analyze the effects of expression of each EFN-4 in specific tissues on SDQL migration. Error bars indicate standard error of proportion of three sample sets, where n=100 animals for each set. ***P<0.005; *P<0.05; n.s., not significant. (C) Confocal micrographs showing EFN-4 immunolocalization in *efn-4* null animals expressing full-length EFN-4 (Ci, Ciii) or EFN-4ΔGPI (Cii, Civ). Maximum intensity *z*-series projections, revealing EFN-4 (Ci) and EFN-4ΔGPI (Cii) expression in *lad-2*-expressing neurons adjacent to the nerve ring (arrow); arrowhead indicates axonal localization of EFN-4. EFN-4ΔGPI immunostaining (Cii) appears qualitatively weaker than for full-length EFN-4 (Ci). This difference is more obvious when viewing a single slice of the *z* series in Ciii and Civ. Arrows indicate EFN-4 localization in individual neurons. Scale bars: 20 µm. (D) A western blot showing results of an immunoprecipitation assay performed on supernatant culture medium (S) or cell lysates (C) of HEK293T cell expressing FLAG::EFN-4ΔGPI using either anti-FLAG (F) or anti-EFN-4 (E) antibodies. The immunoprecipitates were then examined by western blot analysis and probed with anti-FLAG antibodies to visualize the presence of FLAG::EFN-4ΔGPI, marked with an arrow.

EFN-4ΔGPI is sufficient to rescue SDQL axon guidance defects

The ability for EFN-4, a membrane-associated protein, to impact SDQL axon pathfinding when expressed in remote tissues is puzzling. One possible explanation is that EFN-4 functions as a diffusible molecule. To address this, we tested for the ability of a non-membrane-associated form of EFN-4, which lacks the GPI-modification signal sequence (EFN-4ΔGPI), to rescue SDQL axon defects in *efn-4* null animals. Indeed, SDQL defects were rescued with expression of EFN-4ΔGPI, which is comparable with results seen with full-length EFN-4 (Fig. 5B). Strikingly, we also observed significant rescue with EFN-4ΔGPI expressed in the more distant RID and touch receptor mechanosensory neurons (Fig. 5B). Importantly, RID neuron expression of either GPI-linked or EFN-4ΔGPI does not induce ectopic SDQL axon guidance defects in wild-type animals (Fig. 5B). These results suggest that membrane association is not necessary for EFN-4 to mediate axon guidance.

Development (2016) 143, 1182-1191 doi:10.1242/dev.128934

The ability for remote EFN-4ΔGPI expression to rescue *efn-4* SDQL axon guidance defects suggests that EFN-4ΔGPI is diffusible. To test this hypothesis, we compared the localization of EFN-4ΔGPI and EFN-4 in *lad-2*-expressing neurons of *efn-4* transgenic animals via whole-animal immunostaining with antibodies against EFN-4 (Chin-Sang et al., 2002). If EFN-4ΔGPI is not membrane associated and is, in fact, secreted, then we predict that EFN-4ΔGPI immunostaining might be less intense than that of full-length EFN-4 and EFN-4ΔGPI accumulation might be detected outside source cells. Although we did not detect EFN-4ΔGPI accumulation outside *lad-2*-expressing neurons, EFN-4ΔGPI immunodetection in *lad-2*-expressing neurons appeared qualitatively weaker than for full-length EFN-4 (Fig. 5C), consistent with our prediction. One alternative explanation for the weaker signal is that EFN-4ΔGPI is not properly trafficked or folded, thus resulting in protein degradation. In some GPI-linked proteins, loss of GPI modification can lead to aberrant trafficking and degradation, whereas in others, loss of GPI modification results in proteins that are secreted (Campana et al., 2007; Maeda and Kinoshita, 2011; Mayor and Riezman, 2004). To distinguish between the two possibilities, we probed for the presence of FLAG::EFN-4ΔGPI in the culture medium of HEK293T cells expressing FLAG::EFN-4ΔGPI by performing immunoprecipitation on the culture medium with anti-EFN-4 antibodies. Western blot analyses of the immunoprecipitates using an anti-FLAG antibody revealed the presence of FLAG::EFN-4ΔGPI in the medium, demonstrating that EFN-4ΔGPI can be secreted extracellularly. These results, combined with the genetic analyses, support the notion that EFN-4 can function as a soluble diffusible factor to mediate SDQL axon guidance.

SUP-17, the ADAM10 ortholog, might function in EFN-4-mediated axon guidance

The robust rescue of *efn-4*-dependent SDQL axon guidance defects with remote expression of full-length EFN-4 suggests that GPI-linked EFN-4 is released from the cell surface. In vertebrates, GPI-linked ephrins can be released from the cell surface in a regulated fashion by ADAM10- and ADAM12-dependent proteolytic cleavage (Hattori et al., 2000; Janes et al., 2005). As a first approach to determine whether an ADAM regulates EFN-4 proteolytic processing, we examined genetic mutants of *sup-17*, which encodes the *C. elegans* ADAM10 ortholog (Wen et al., 1997), for SDQL migration defects. Although loss of *sup-17* results in arrested embryonic development, *sup-17* exhibits maternal activity that partially rescues embryonic lethality of *sup-17* null alleles (Tax et al., 1997). We examined viable, maternally rescued *sup-17* null and hypomorphic animals and identified modest but significant levels of SDQL axon pathfinding defects (Fig. 6), indicating an axon guidance role for SUP-17.

In addition to ephrins, ADAM10 can proteolytically cleave multiple different substrates, including ligands for the epidermal growth factor receptor, adhesion molecules and Notch receptors (Hartmann et al., 2002; Pruessmeyer and Ludwig, 2009; Sahin et al., 2004). Previous genetic analyses of *sup-17* support a role for SUP-17 in processing LIN-12/Notch in *C. elegans* (Jarriault and Greenwald, 2005; Tax et al., 1997; Wen et al., 1997). Thus, the SDQL neuron defects observed in *sup-17* animals might result from defective processing of one or more SUP-17 substrates. To ascertain whether defective EFN-4 processing contributes to this *sup-17* SDQL cell migration defect, we tested the ability for EFN-4ΔGPI to rescue *sup-17* SDQL defects (Fig. 6). Indeed, SDQL-specific expression of EFN-4ΔGPI but not full-length EFN-4 rescued abnormal SDQL defects in *sup-17* hypomorphic animals. Similarly, EFN-4ΔGPI but not full-length EFN-4 expressed in the more distant RID neuron rescues SDQL defects in *sup-17* null animals. Surprisingly, we did not observe rescue with SDQL expression of EFN-4ΔGPI in *sup-17* null animals as we did in the hypomorphic animals, despite the fact that the EFN-4ΔGPI transgenes are common in both strains. The reason for this is not clear, but the positive rescue we observed reveals the ability for a putative soluble form of EFN-4 to bypass SUP-17 function, consistent with the notion that SUP-17 functions in the processing of EFN-4. Because SDQL defects in *sup-17* null animals are less penetrant than in *efn-4* null animals, there are likely to be additional mechanisms underlying EFN-4 processing, Moreover, the modest rescue by RID neuron expression of EFN-4ΔGPI in *sup-17* null animals suggests that SUP-17 probably also promotes SDQL axon guidance through EFN-4-independent pathways.

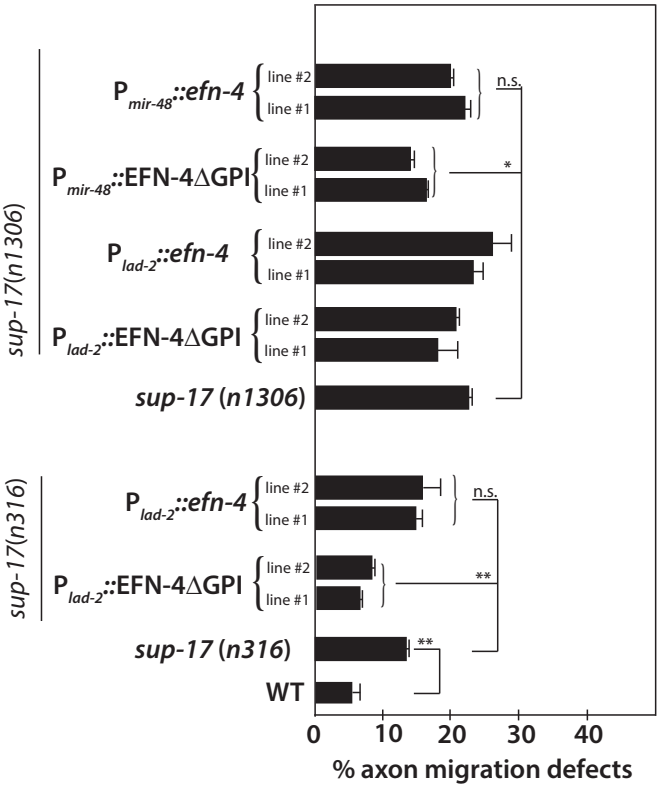

Fig. 6. SUP-17 might function in EFN-4 processing. Quantitation of SDQL defects in *sup-17*(*n316*) and *sup-17*(*n1306*) mutant backgrounds expressing EFN-4ΔGPI or full-length EFN-4. We examined two independent transgenic lines to analyze the effects of expression of each EFN-4 form in specific tissues on SDQL migration. Error bars indicate standard error of proportion of three sample sets, where *n*=100 animals for each set. ***P*<0.01; **P*<0.05; n.s., not significant.

DISCUSSION

We report a novel role for ephrin EFN-4 in *C. elegans* axon guidance. Our data suggest that EFN-4 acts as a soluble factor to direct axon pathfinding via LAD-2, which probably functions as a non-canonical receptor for EFN-4.

EFN-4 can act as a long-range axon guidance factor

Ephrins, both GPI-linked and transmembrane forms, typically function as short-range cues to mediate cell repulsion in a juxtacrine

Development (2016) 143, 1182-1191 doi:10.1242/dev.128934

fashion. After forming *trans* interactions with cognate Eph receptors, bound ephrins undergo regulated proteolytic cleavage by ADAMs. This cleavage of ephrin severs the ephrin-Eph-mediated cell-cell contact, thus resulting in cell repulsion (Hattori et al., 2000; Janes et al., 2005).

Our study reveals that GPI-linked EFN-4 also functions in axon guidance. But our data are consistent with EFN-4 acting as a soluble diffusible factor. Indeed, provision of EFN-4ΔGPI in *efn-4* mutant animals, even in tissues distant from SDQL, is sufficient to rescue SDQL cell defects, demonstrating that membrane association is not required for EFN-4 function and that EFN-4 probably functions as a soluble diffusible factor. In support of this hypothesis, we demonstrate that EFN-4ΔGPI expressed in cultured HEK293 cells can be secreted extracellularly.

Interestingly, soluble forms of mammalian GPI-linked ephrins were recently found to be produced by glioblastoma multiforme tumor cells when cultured *ex vivo*. In these studies, soluble forms of ephrin A1 were released from these cells in a matrix metalloprotease-dependent manner and are independent of cell-cell contact. Moreover, when cultured cells, including embryonic neurons, were exposed to soluble ephrin A1-conditioned medium, diverse physiological changes were observed, including growth cone collapse and attenuated cell migration (Beauchamp et al., 2012; Wykosky et al., 2008). These studies, combined with our results, reveal that conserved ephrin-mediated processes probably include the use of endogenous soluble ephrins acting as diffusible factors.

These findings raise additional questions. How is soluble EFN-4 distributed? Do other EFN-4-mediated processes, such as male tail and epidermal morphogenesis, also utilize soluble EFN-4? How is GPI-linked EFN-4 released from the plasma membrane?

The ability for EFN-4ΔGPI, but not full-length EFN-4, to rescue SDQL defects in *sup-17* mutant animals suggests that the SUP-17 ADAM protease functions in EFN-4 processing to free EFN-4 from the plasma membrane. However, the less-penetrant SDQL axon defect in *sup-17* versus *efn-4* null animals suggests that SUP-17 is not the only protein to process EFN-4. Likewise, the modest or lack of SDQL rescue in *sup-17* null animals with EFN-4ΔGPI suggests that the axon guidance defects in these animals might be due to abnormal processing of additional *sup-17* substrates besides EFN-4. Perhaps, these other substrates function together with EFN-4, thus accounting for the poorer rescue of SDQL defects in *sup-17* null compared with the *sup-17* hypomorphic background.

EFN-4: guidance cue or permissive factor?

The ability for EFN-4 expression in multiple tissues to rescue SDQL axon pathfinding in *efn-4* null animals indicates that EFN-4 can function both cell autonomously and non-cell autonomously. Of the tissues tested, EFN-4 expression in hyp7 cells produces the weakest rescue (Fig. 4B), a surprising result considering that SDQL neurons are in contact with hyp7 neurons throughout axon navigation. It is not clear what the underlying reason is but we attribute this to probable low EFN-4 expression in the *dpy-7* promoter-driven transgenic lines. In our experience, animals are sensitive to the apparent toxicity of transgenes that utilize the *dpy-7* promoter to drive gene expression (L.C., unpublished results); as such, low sub-lethal concentrations of the $P_{dpy\text{-}7}$::*efn-4* construct were used to generate transgenic *efn-4* animal expressing *efn-4* in hyp7 neurons (see the Materials and Methods).

Does EFN-4 function as a repulsive or attractive guidance cue? In addition to strong EFN-4 expression in the head and tail neurons, robust EFN-4 expression is seen in the ventral nerve cord (Chin-Sang et al., 2002; Fig. S1). On the basis of this expression pattern and the dorsal-ward extension of the wild-type SDQL axon to the dorsal sublateral cord, one would predict that EFN-4 functions as a repulsive cue. Supporting this notion, ventral EFN-4 expression in the touch receptor mechanosensory neurons rescues SDQL defects in *efn-4* animals. If EFN-4 does indeed function as a repulsive cue, one would predict that dorsal EFN-4 expression would enhance SDQL axon guidance defects in *efn-4* animals. Contrary to this prediction, dorsal EFN-4 expression in the RID neuron does not enhance *efn-4* SDQL defects but instead, rescues it, suggesting that EFN-4 acts as an attractive cue. Consistent with EFN-4 functioning as an attractive cue, we observed a modest but statistically significant SDQL axon defect with ventral EFN-4 expression in wild-type animals.

Axon navigation is a complex process that relies on the ability for a neuron to integrate, interpret and respond to the signals of multiple cues encountered during its navigation. For example, whether a neuron responds to UNC-6 netrin as a repulsive or positive cue depends not only on the netrin receptors present on the growth cone, but also the presence of other guidance cues and extrinsic factors, including UNC-129 that can influence the sensitivity of the UNC-6 receptors or mask the UNC-6 signal (Kim et al., 1999; MacNeil et al., 2009). Thus the response of SDQL to ectopic EFN-4 might be influenced by the strength and the temporal activity of the promoters used to drive EFN-4 expression. An alternative explanation for the SDQL rescue with both dorsal and ventral EFN-4 expression is that EFN-4 functions as a permissive factor, rather than a guidance cue. Supporting this possibility is the robust rescue of SDQL defects in *efn-4* animals with EFN-4 expression in multiple tissues that are adjacent or distant to SDQL.

LAD-2 as a non-canonical ephrin receptor

Our genetic analysis reveals that VAB-1 functions in axon guidance of *lad-2*-expressing neurons. However, the higher penetrance of SDQL axon defects in *efn-4* null animals compared with *vab-1* null animals indicates that EFN-4 can mediate axon guidance independent of VAB-1. This finding is not surprising based on the previous discovery that EFN-4 has VAB-1-independent roles in epidermal morphogenesis and axon branching (Chin-Sang et al., 2002; Schwieterman et al., 2016). Our study identifies LAD-2 as a likely receptor for EFN-4 in axon guidance. Consistent with EFN-4 and LAD-2 having a ligand-receptor relationship, *efn-4* and *lad-2* both function in the same genetic pathway and EFN-4 can biochemically interact with LAD-2.

The mammalian L1CAMs, L1 and CHL1, were recently shown to function in ephrin-Eph-mediated retinal ganglion and thalamocortical axon pathfinding (Dai et al., 2012; Demyanenko et al., 2011b). These studies demonstrate that L1 and CHL1 biochemically interact with the corresponding Eph receptors, which can regulate the phosphorylation state of L1 to modulate axon guidance. Thus, Eph receptors are required for mammalian L1CAMs to mediate pathfinding of these axons. This mechanism might also be conserved in *C. elegans* because our genetic analysis reveals that *vab-1* functions in the same pathway as *lad-2*. However, the weaker penetrance of axon defects in *vab-1* versus *efn-4* and *lad-2* null animals suggest that LAD-2 and EFN-4 can also function independently of VAB-1. It is unclear whether this VAB-1-independent LAD-2 function is also conserved with mammalian L1CAMs. Given that both LAD-2 and mammalian L1CAMs are conserved semaphorin co-receptors (Castellani et al., 2000, 2004; Demyanenko et al., 2011a; Falk et al., 2005; Wang et al., 2008), we surmise that this is likely.

Development (2016) 143, 1182-1191 doi:10.1242/dev.128934

How do EFN-4 and LAD-2 mediate axon guidance? Our data support a role for EFN-4 as a soluble diffusible factor that functions in a separate pathway from MAB-20 and PLX-2. On the basis of these findings, we propose three simple models for how EFN-4 facilitates LAD-2-mediated axon guidance. The first model postulates that LAD-2 acts as a receptor for EFN-4, which acts as a guidance cue that provides an additional signal to MAB-20 to direct SDQL axon guidance. The second model proposes that EFN-4 functions as a permissive factor and that EFN-4 binding to LAD-2 potentiates the ability for LAD-2 to more efficiently transmit a MAB-20 guidance signal or additional as-yet-unidentified guidance cues, perhaps by influencing LAD-2 conformation. Alternatively, soluble EFN-4 could act as a permissive factor by being deposited along the extracellular matrix and facilitating adhesion of the migrating SDQL axon via LAD-2. These latter two models, which might not be mutually exclusive, require that soluble EFN-4 has a relatively high diffusion rate and/or that low extracellular EFN-4 concentration is sufficient. Further analysis will have to be performed to test the validity of these models.

How does LAD-2 function as a receptor, particularly because LAD-2 does not harbor obvious catalytic domains or conserved motifs in the cytoplasmic tail that could link LAD-2 to a signal transduction pathway? As LAD-2 functions to bridge MAB-20 to PLX-2 (Wang et al., 2008), LAD-2 might similarly act as a co-receptor to link EFN-4 to an as-yet-unidentified receptor. An alternative possibility is that LAD-2 can, in fact, function as a receptor to mediate EFN-4 signals intracellularly by as-yet-unknown mechanisms. Additional studies will have to be performed to distinguish these two possibilities.

MATERIALS AND METHODS

Strains

C. elegans strains, provided by the *Caenorhabditis* Genetics Center, were grown on nematode growth medium (NGM) plates at 21°C. N2 Bristol served as the wild-type strain (Brenner, 1974). The alleles used in this study are listed by linkage groups as follows: LGI: *sup-17*(*n316*), *sup-17*(*n1306*) (Tax et al., 1997), *mab-20*(*ev574*); LGII: *vab-1*(*dx31*) (George et al., 1998), *plx-2*(*ev773*); LGIV: *efn-4*(*bx80*) (Chin-Sang et al., 2002), *lad-2*(*tm3056*) (Wang et al., 2008).

C. elegans expression vectors and generation of transgenic animals

Transgenic animals were generated according to standard procedures (Mello et al., 1991). We injected *efn-4*(*bx80*), *sup-17*(*n316*) and *sup-17*(*n1306*) *unc-29*(*e1072*)/hT2[*qIs48*] with the following *efn-4* expression constructs with 50 ng/µl P*lad-2*::*gfp* as a co-injection marker that also allows visualization of SDQL. The concentration of the *efn-4* expression constructs used to generate transgenic animals is listed below.

P*lad-2*::*gfp* (pLC373): 9 kb of *lad-2* sequences upstream of the start codon was PCR-amplified and subcloned into pBSII KS- together with GFP coding sequence and *lad-2* 3′UTR. Injected as a co-injection marker at 50 ng/µl. P*efn-4*::*efn-4* (pLC667): *efn-4* genomic DNA was amplified by PCR and cloned between the *Not*I and *Eco*RV sites of pBS II KS- (Chin-Sang et al., 2002). Injected at 20 ng/µl. P*lad-2*::*efn-4* (pLC670): subcloned into pBSII KS-, 9 kb of *lad-2* upstream sequence was subcloned together with *efn-4* genomic sequence that was amplified from pLC667 at the start codon (Wang et al., 2008). Injected at 20 ng/µl. P*dpy-7*::*efn-4* (pLC678): promoter sequence of pLC667 was replaced with PCR-amplified *dpy-7* promoter fragment (Gilleard et al., 1997). Injected at 2.5 ng/µl. P*myo-3*::*efn-4* (pLC681): promoter sequence of pLC667 was replaced with PCR-amplified *myo-3* promoter fragment (Okkema et al., 1993). Injected at 15 ng/µl. P*mir-48*::*efn-4* (pLC688): promoter sequence of pLC667 was replaced with PCR-amplified *mir-48* promoter fragment (Li et al., 2005). Injected at 20 ng/µl. P*mec-7*::*efn-4* (pLC692): Promoter sequence of pLC667 was replaced with PCR-amplified *mec-7* promoter fragment (Kim et al., 1999). Injected at 20 ng/µl. P*lad-2*::EFN-4ΔGPI (pLC686): the *efn-4* sequence of pLC670 was truncated following amino acid 327, thereby deleting the GPI signal sequence. A stop codon was inserted after the amino acid 327. Injected at 20 ng/µl. P*mir-48*::EFN-4ΔGPI (pLC710): promoter sequence of pLC686 was replaced with *mir-48* promoter fragment. Injected at 20 ng/µl. P*mec-7*::EFN-4ΔGPI (pLC709): Promoter sequence of pLC686 was replaced with *mec-7* promoter fragment. Injected at 20 ng/µl.

Phenotypic analysis of SMD, PLN, SDQR and SDQL axons

Young adult animals were mounted on 2% agarose pads, paralyzed in M9 buffer containing 10 mM levamisole and examined using an Axioplan 2 microscope (Carl Zeiss). The SDQL axon was scored as having a migration defect if it migrated ventrally at the second dorsal turn. This phenotype is distinct from the bipolar phenotype, which was scored as such if the SDQL neuron extended two axons. Three sample sets were analyzed for each genetic strain, where n=100 for each sample set. Statistical analysis was performed using ANOVA followed by *post hoc* pairwise Student's t-test with Bonferroni correction. Confocal micrographs of SDQL axons in different genetic backgrounds in Fig. 1 were taken using the 40× objective of an Olympus Fluoview FV1000 upright confocal microscope. Images were collected as stacks along the z-axis. Shown are maximum intensity projections obtained using the Fluoview software.

To examine SDQL phenotypes in the *sup-17*(*n1306*) null background, we performed all manipulations in the *sup-17*(*n1306*) *unc-29*(*e1072*)/hT2 [*qIs48*] animals. We then examined viable homozygous *sup-17*(*n1306*) *unc-29*(*e1072*) animals, which are uncoordinated because of the closely linked *unc-29* mutation and lack the green pharynx found in the P*myo-2*::GFP-carrying *hT2[qIs48]* balancer chromosome. *unc-29* encodes an acetylcholine receptor subunit and does not have a reported role in axon guidance (Fleming et al., 1997).

Immunofluorescence

Animals were fixed and stained for indirect immunofluorescence using the freeze-crack methanol fixation method (Chen et al., 2001). EFN-4 polyclonal antibodies (Chin-Sang et al., 2002) were used at 1:200 dilution. Secondary antibodies (Alexa Fluor 488 and 568, Molecular Probes) were used at 1:500 dilution.

Mammalian cell expression vectors

pCMV::LAD-2::HA (pLC669): *lad-2* cDNA was PCR-amplified with a primer-encoded HA tag and cloned into pCDNA3.1/Myc HisB between the *Eco*RI and *Eco*RV sites. pCMV::FLAG::EFN-4 (pLC642): *efn-4* cDNA was cloned into 3xFLAG-CMV 7.1 between the *Eco*RI and *Eco*RV sites. pCMV::FLAG::EFN-4ΔGPI (pLC 707): *efn-4* cDNA was PCR-amplified using primers that remove the last 29 amino acids of EFN-4 containing the GPI modification sequence and cloned in 3xFLAG-CMV 7.1 between the *Eco*RI and *Eco*RV sites. LAD-2ECD::AP (pLC714): *lad-2* cDNA was truncated following amino acid 1126 and cloned into vector pAPtag-2 (GenHunter) between the *Hin*DIII and *Bgl*II sites.

Fc-MycHis (pMH180): Fc open reading frame was PCR-amplified from plasmid pCXFc-KAL (Bulow et al., 2002) and subcloned into pSecTagA (Life Technologies) between the *Hin*dIII and *Eco*RI sites. EFN-4ΔGPI-Fc-MycHis (pMH874): EFN-4 cDNA was PCR-amplified with the following primers so that the first 26 amino acids, which form the secretion signal, as well as the last 22 amino acids, which constitute the GPI modification signal, are not included. This PCR product was subcloned using Gibson Assembly (New England BioLabs) into *Hin*dIII-linearized pMH180. Forward primer: AGGCGCGCCGTACGAAGcttAGACGAGCACATTGTCTAC; reverse primer: AAAATCCTTGGAATATTtAAGcttCGACAAAACTCACACA.

Cell culture and transfection

HEK293T cells were maintained in Dulbecco's modified Eagle's medium (DMEM) (Caisson Laboratories and Mediatech) supplemented with 10% ultra-low IgG fetal bovine serum (Life Technologies), 1 mM L-glutamine (Caisson Laboratories Inc.), and 1× penicillin-streptomycin (Caisson Laboratories). HEK293T cells were transfected with LipofectAMINE 2000 Transfection Reagent (Life Technologies) and Opti-MEM Reduced Serum

Development (2016) 143, 1182-1191 doi:10.1242/dev.128934

Medium (Life Technologies) according to the manufacturer's protocol. Final DNA concentrations were 10 ng/µl. Transfections were incubated at 37°C in 5% CO_2 atmosphere for 40-48 h. Cells that were transfected for co-immunoprecipitation assays were isolated and washed with PBS. For cells that were transfected for BLI analysis, supernatants were harvested, centrifuged to remove cellular debris, then used directly or concentrated using a 10 kDa cut-off filter (Centricon). Protein production was confirmed by either western blotting to detect Myc tags of the transfected ephrin-Fc proteins, or by AP-turnover assay for LAD-2ECD::AP. For cells that were transfected to assess secretion of EFN-4ΔGPI, the supernatants were collected at 48 h and for three subsequent days, concentrated using Amicon Ultra-15 filter devices (Millipore), and subjected to immunoprecipitation with EFN-4 polyclonal antibodies (Chin-Sang et al., 2002).

Co-immunoprecipitation assays

200-500 µl of cell lysate was incubated with NETN buffer (20 mM Tris-HCl, pH 8, 100 mM NaCl, 1 mM EDTA and 0.5% NP-40) containing an anti-FLAG M2 monoclonal antibody (Sigma-Aldrich, F1804; 1 µg) or anti-Myc polyclonal antibody (Covance, 9E10; 1 µg) or anti-SAX-7 polyclonal antibody (6991; Chen et al., 2001; 1 µg) at 4°C for 4 h followed by an incubation with 20 µl protein A/G beads (Santa Cruz Biotechnology) for 2 h or overnight. The beads were then washed three times with NETN lysis buffer.

Western blot analysis and reagents

Cell lysates prepared in NETN buffer containing 1 mM NaF, 2.5 mM β-glycerophosphate and a protease inhibitor cocktail (Life Technologies). Protein concentrations were determined with the Bio-Rad protein assay (Bio-Rad). Proteins in cell lysates were resolved by SDS-PAGE and electrophoretically transferred to nitrocellulose membrane. Membranes were processed as described in Wang et al. (2008). Primary antibodies used included anti-FLAG M2 (Sigma-Aldrich, 16B12; 1:1000), anti-Myc (Covance, 9E10;1:1000) and anti-HA (Covance, MMS-101P; 1:1000).

Biolayer interferometry (BLI)

Biolayer interferometry measurements were made on a FortéBio Octet-QK instrument using anti-human IgG Fc capture (AHC) biosensors. Assays of 200 µl volumes were performed in 96-well microplates at 25°C. Biosensors were conditioned for 3 min in Opti-MEM medium prior to loading. Ephrin-Fc ligands or Fc controls were bound onto the AHC biosensors for 60 min then a baseline was established in Opti-MEM for 15 min. Sensors were then incubated in LAD-2ECD::AP tissue culture supernatant for 60 min (analyte association phase), followed by incubation in Opti-MEM for 60 min (dissociation phase).

Acknowledgements

We thank Andrew Chisholm and Ian Chin-Sang for sharing *efn-4* expression constructs, transgenic strains and EFN-4 antibodies, the *Caenorhabditis* Genetic Center (supported by the National Institutes of Health, NIH P40-OD01440) for strains used in this study, and Ann Rougvie for intellectual and editorial advice.

Competing interests

The authors declare no competing or financial interests.

Author contributions

L.C. conceived the project, designed experiments, analyzed data, and wrote the manuscript; B.D. performed the majority of the experiments; M.M.-A. performed many of the genetic and co-immunoprecipitation experiments; M.L.H. and J.L.M. designed BLI experiments and analyzed BLI data; A.A.S. and C.J.D. performed BLI experiments and analyzed BLI data.

Funding

This work is supported in part by Kennesaw State University's Center for Excellence in Teaching and Learning and the Office of the Vice President for Research to M.L.H. and by the National Institutes of Health [R15 GM080701 to J.M. and RO1 NS045873 to L.C.]. Deposited in PMC for release after 12 months.

Supplementary information

Supplementary information available online at
http://dev.biologists.org/lookup/suppl/doi:10.1242/dev.128934/-/DC1

References

Abdiche, Y., Malashock, D., Pinkerton, A. and Pons, J. (2008). Determining kinetics and affinities of protein interactions using a parallel real-time label-free biosensor, the Octet. *Anal. Biochem.* **377**, 209-217.

Beauchamp, A., Lively, M. O., Mintz, A., Gibo, D., Wykosky, J. and Debinski, W. (2012). EphrinA1 is released in three forms from cancer cells by matrix metalloproteases. *Mol. Cell. Biol.* **32**, 3253-3264.

Boulin, T., Pocock, R. and Hobert, O. (2006). A novel Eph receptor-interacting IgSF protein provides *C. elegans* motoneurons with midline guidepost function. *Curr. Biol.* **16**, 1871-1883.

Brenner, S. (1974). The genetics of Caenorhabditis elegans. *Genetics* **77**, 71-94.

Bulow, H. E., Berry, K. L., Topper, L. H., Peles, E. and Hobert, O. (2002). Heparan sulfate proteoglycan-dependent induction of axon branching and axon misrouting by the Kallmann syndrome gene kal-1. *Proc. Natl. Acad. Sci. USA* **99**, 6346-6351.

Campana, V., Caputo, A., Sarnataro, D., Paladino, S., Tivodar, S. and Zurzolo, C. (2007). Characterization of the properties and trafficking of an anchorless form of the prion protein. *J. Biol. Chem.* **282**, 22747-22756.

Castellani, V., Chédotal, A., Schachner, M., Faivre-Sarrailh, C. and Rougon, G. (2000). Analysis of the L1-deficient mouse phenotype reveals cross-talk between Sema3A and L1 signaling pathways in axonal guidance. *Neuron* **27**, 237-249.

Castellani, V., Falk, J. and Rougon, G. (2004). Semaphorin3A-induced receptor endocytosis during axon guidance responses is mediated by L1 CAM. *Mol. Cell. Neurosci.* **26**, 89-100.

Chen, L. and Zhou, S. (2010). "CRASH"ing with the worm: insights into L1CAM functions and mechanisms. *Dev. Dyn.* **239**, 1490-1501.

Chen, L., Ong, B. and Bennett, V. (2001). LAD-1, the *Caenorhabditis elegans* L1CAM homologue, participates in embryonic and gonadal morphogenesis and is a substrate for fibroblast growth factor receptor pathway-dependent phosphotyrosine-based signaling. *J. Cell Biol.* **154**, 841-855.

Chin-Sang, I. D., George, S. E., Ding, M., Moseley, S. L., Lynch, A. S. and Chisholm, A. D. (1999). The ephrin VAB-2/EFN-1 functions in neuronal signaling to regulate epidermal morphogenesis in C. elegans. *Cell* **99**, 781-790.

Chin-Sang, I. D., Moseley, S. L., Ding, M., Harrington, R. J., George, S. E. and Chisholm, A. D. (2002). The divergent *C. elegans* ephrin EFN-4 functions inembryonic morphogenesis in a pathway independent of the VAB-1 Eph receptor. *Development* **129**, 5499-5510.

Dai, J., Dalal, J. S., Thakar, S., Henkemeyer, M., Lemmon, V. P., Harunaga, J. S., Schlatter, M. C., Buhusi, M. and Maness, P. F. (2012). EphB regulates L1 phosphorylation during retinocollicular mapping. *Mol. Cell. Neurosci.* **50**, 201-210.

Demyanenko, G. P., Riday, T. T., Tran, T. S., Dalal, J., Darnell, E. P., Brennaman, L. H., Sakurai, T., Grumet, M., Philpot, B. D. and Maness, P. F. (2011a). NrCAM deletion causes topographic mistargeting of thalamocortical axons to the visual cortex and disrupts visual acuity. *J. Neurosci.* **31**, 1545-1558.

Demyanenko, G. P., Siesser, P. F., Wright, A. G., Brennaman, L. H., Bartsch, U., Schachner, M. and Maness, P. F. (2011b). L1 and CHL1 cooperate in thalamocortical axon targeting. *Cereb. Cortex* **21**, 401-412.

Egea, J. and Klein, R. (2007). Bidirectional Eph-ephrin signaling during axon guidance. *Trends Cell Biol.* **17**, 230-238.

Falk, J., Bechara, A., Fiore, R., Nawabi, H., Zhou, H., Hoyo-Becerra, C., Bozon, M., Rougon, G., Grumet, M., Püschel, A. W. et al. (2005). Dual functional activity of semaphorin 3B is required for positioning the anterior commissure. *Neuron* **48**, 63-75.

Fire, A. and Waterston, R. H. (1989). Proper expression of myosin genes in transgenic nematodes. *EMBO J.* **8**, 3419-3428.

Fleming, J. T., Squire, M. D., Barnes, T. M., Tornoe, C., Matsuda, K., Ahnn, J., Fire, A., Sulston, J. E., Barnard, E. A., Sattelle, D. B. et al. (1997). *Caenorhabditis elegans* levamisole resistance genes lev-1, unc-29, and unc-38 encode functional nicotinic acetylcholine receptor subunits. *J. Neurosci.* **17**, 5843-5857.

George, S. E., Simokat, K., Hardin, J. and Chisholm, A. D. (1998). The VAB-1 Eph receptor tyrosine kinase functions in neural and epithelial morphogenesis in *C. elegans*. *Cell* **92**, 633-643.

Gilleard, J. S., Barry, J. D. and Johnstone, I. L. (1997). cis regulatory requirements for hypodermal cell-specific expression of the *Caenorhabditis elegans* cuticle collagen gene dpy-7. *Mol. Cell. Biol.* **17**, 2301-2311.

Grossman, E. N., Giurumescu, C. A. and Chisholm, A. D. (2013). Mechanisms of ephrin receptor protein kinase-independent signaling in amphid axon guidance in *Caenorhabditis elegans*. *Genetics* **195**, 899-913.

Hartmann, D., de Strooper, B., Serneels, L., Craessaerts, K., Herreman, A., Annaert, W., Umans, L., Lubke, T., Lena Illert, A., von Figura, K. et al. (2002). The disintegrin/metalloprotease ADAM 10 is essential for Notch signalling but not for alpha-secretase activity in fibroblasts. *Hum. Mol. Genet.* **11**, 2615-2624.

Hattori, M., Osterfield, M. and Flanagan, J. G. (2000). Regulated cleavage of a contact-mediated axon repellent. *Science* **289**, 1360-1365.

Helmbacher, F., Schneider-Maunoury, S., Topilko, P., Tiret, L. and Charnay, P. (2000). Targeting of the EphA4 tyrosine kinase receptor affects dorsal/ventral pathfinding of limb motor axons. *Development* **127**, 3313-3324.

Hornberger, M. R., Dütting, D., Ciossek, T., Yamada, T., Handwerker, C., Lang, S., Weth, F., Huf, J., Wessel, R., Logan, C. et al. (1999). Modulation of EphA receptor function by coexpressed ephrinA ligands on retinal ganglion cell axons. *Neuron* **22**, 731-742.

Ikegami, R., Zheng, H., Ong, S.-H. and Culotti, J. (2004). Integration of semaphorin-2A/MAB-20, ephrin-4, and UNC-129 TGF-beta signaling pathways regulates sorting of distinct sensory rays in *C. elegans*. *Dev. Cell* **6**, 383-395.

Janes, P. W., Saha, N., Barton, W. A., Kolev, M. V., Wimmer-Kleikamp, S. H., Nievergall, E., Blobel, C. P., Himanen, J.-P., Lackmann, M. and Nikolov, D. B. (2005). Adam meets Eph: an ADAM substrate recognition module acts as a molecular switch for ephrin cleavage in trans. *Cell* **123**, 291-304.

Jarriault, S. and Greenwald, I. (2005). Evidence for functional redundancy between *C. elegans* ADAM proteins SUP-17/Kuzbanian and ADM-4/TACE. *Dev. Biol.* **287**, 1-10.

Kao, T.-J. and Kania, A. (2011). Ephrin-mediated cis-attenuation of Eph receptor signaling is essential for spinal motor axon guidance. *Neuron* **71**, 76-91.

Kim, S., Ren, X. C., Fox, E. and Wadsworth, W. G. (1999). SDQR migrations in *Caenorhabditis elegans* are controlled by multiple guidance cues and changing responses to netrin UNC-6. *Development* **126**, 3881-3890.

Li, M., Jones-Rhoades, M. W., Lau, N. C., Bartel, D. P. and Rougvie, A. E. (2005). Regulatory mutations of mir-48, a *C. elegans* let-7 family MicroRNA, cause developmental timing defects. *Dev. Cell* **9**, 415-422.

Luria, V., Krawchuk, D., Jessell, T. M., Laufer, E. and Kania, A. (2008). Specification of motor axon trajectory by ephrin-B:EphB signaling: symmetrical control of axonal patterning in the developing limb. *Neuron* **60**, 1039-1053.

MacNeil, L. T., Hardy, W. R., Pawson, T., Wrana, J. L. and Culotti, J. G. (2009). UNC-129 regulates the balance between UNC-40 dependent and independent UNC-5 signaling pathways. *Nat. Neurosci.* **12**, 150-155.

Maeda, Y. and Kinoshita, T. (2011). Structural remodeling, trafficking and functions of glycosylphosphatidylinositol-anchored proteins. *Prog. Lipid Res.* **50**, 411-424.

Mayor, S. and Riezman, H. (2004). Sorting GPI-anchored proteins. *Nat. Rev. Mol. Cell Biol.* **5**, 110-120.

Mello, C. C., Kramer, J. M., Stinchcomb, D. and Ambros, V. (1991). Efficient gene transfer in *C.elegans*: extrachromosomal maintenance and integration of transforming sequences. *EMBO J.* **10**, 3959-3970.

Mohamed, A. M. and Chin-Sang, I. D. (2006). Characterization of loss-of-function and gain-of-function Eph receptor tyrosine kinase signaling in *C. elegans* axon targeting and cell migration. *Dev. Biol.* **290**, 164-176.

Nakao, F., Hudson, M. L., Suzuki, M., Peckler, Z., Kurokawa, R., Liu, Z., Gengyo-Ando, K., Nukazuka, A., Fujii, T., Suto, F. et al. (2007). The PLEXIN PLX-2 and the ephrin EFN-4 have distinct roles in MAB-20/Semaphorin 2A signaling in *Caenorhabditis elegans* morphogenesis. *Genetics* **176**, 1591-1607.

Okkema, P. G., Harrison, S. W., Plunger, V., Aryana, A. and Fire, A. (1993). Sequence requirements for myosin gene expression and regulation in *Caenorhabditis elegans*. *Genetics* **135**, 385-404.

Pruessmeyer, J. and Ludwig, A. (2009). The good, the bad and the ugly substrates for ADAM10 and ADAM17 in brain pathology, inflammation and cancer. *Semin. Cell Dev. Biol.* **20**, 164-174.

Rashid, T., Upton, A. L., Blentic, A., Ciossek, T., Knöll, B., Thompson, I. D. and Drescher, U. (2005). Opposing gradients of ephrin-As and EphA7 in the superior colliculus are essential for topographic mapping in the mammalian visual system. *Neuron* **47**, 57-69.

Sahin, U., Weskamp, G., Kelly, K., Zhou, H.-M., Higashiyama, S., Peschon, J., Hartmann, D., Saftig, P. and Blobel, C. P. (2004). Distinct roles for ADAM10 and ADAM17 in ectodomain shedding of six EGFR ligands. *J. Cell Biol.* **164**, 769-779.

Sasakura, H., Inada, H., Kuhara, A., Fusaoka, E., Takemoto, D., Takeuchi, K. and Mori, I. (2005). Maintenance of neuronal positions in organized ganglia by SAX-7, a *Caenorhabditis elegans* homologue of L1. *EMBO J.* **24**, 1477-1488.

Schwarz, V., Pan, J., Voltmer-Irsch, S. and Hutter, H. (2009). IgCAMs redundantly control axon navigation in *Caenorhabditis elegans*. *Neural Dev.* **4**, 13.

Schwieterman, A. A., Steves, A. N., Yee, V., Donelson, C. J., Bentley, M. R., Santorella, E. M., Mehlenbacher, T. V., Pital, A., Howard, A. M., Wilson, M. R. et al. (2016). The *Caenorhabditis elegans* Ephrin EFN-4 functions non-cell autonomously with heparan sulfate proteoglycans to promote axon outgrowth and branching. *Genetics* **202**, 639-660.

Tax, F. E., Thomas, J. H., Ferguson, E. L. and Horvitz, H. R. (1997). Identification and characterization of genes that interact with lin-12 in *Caenorhabditis elegans*. *Genetics* **147**, 1675-1695.

Wang, X., Roy, P. J., Holland, S. J., Zhang, L. W., Culotti, J. G. and Pawson, T. (1999). Multiple ephrins control cell organization in *C. elegans* using kinase-dependent and -independent functions of the VAB-1 Eph receptor. *Mol. Cell* **4**, 903-913.

Wang, H., Chadaram, S. R., Norton, A. S. and Laskowski, M. B. (2001). Development of inhibition by ephrin-A5 on outgrowth of embryonic spinal motor neurites. *J. Neurobiol.* **47**, 233-243.

Wang, X., Kweon, J., Larson, S. and Chen, L. (2005). A role for the *C. elegans* L1CAM homologue lad-1/sax-7 in maintaining tissue attachment. *Dev. Biol.* **284**, 273-291.

Wang, X., Zhang, W., Cheever, T., Schwarz, V., Opperman, K., Hutter, H., Koepp, D. and Chen, L. (2008). The *C. elegans* L1CAM homologue LAD-2 functions as a coreceptor in MAB-20/Sema2–mediated axon guidance. *J. Cell Biol.* **180**, 233-246.

Wartchow, C. A., Podlaski, F., Li, S., Rowan, K., Zhang, X., Mark, D. and Huang, K.-S. (2011). Biosensor-based small molecule fragment screening with biolayer interferometry. *J. Comput. Aided Mol. Des.* **25**, 669-676.

Wen, C., Metzstein, M. M. and Greenwald, I. (1997). SUP-17, a *Caenorhabditis elegans* ADAM protein related to Drosophila KUZBANIAN, and its role in LIN-12/NOTCH signalling. *Development* **124**, 4759-4767.

White, J. G., Southgate, E., Thomson, J. N. and Brenner, S. (1986). The structure of the nervous system of the nematode *Caenorhabditis elegans*. *Philos. Trans. R. Soc. Lond. B Biol. Sci.* **314**, 1-340.

Wilson, J. L., Scott, I. M. and McMurry, J. L. (2010). Optical biosensing: kinetics of protein A-IGG binding using biolayer interferometry. *Biochem. Mol. Biol. Educ.* **38**, 400-407.

Wykosky, J., Palma, E., Gibo, D. M., Ringler, S., Turner, C. P. and Debinski, W. (2008). Soluble monomeric EphrinA1 is released from tumor cells and is a functional ligand for the EphA2 receptor. *Oncogene* **27**, 7260-7273.